

PROGRESS WITH THE DIAMOND-II STORAGE RING LATTICE

H. Ghasem[†], I. P. S. Martin, B. Singh, Diamond Light Source, Oxfordshire, UK

Abstract

Building on the CDR proposal for the Diamond-II storage ring [1], a number of changes have been implemented to improve the performance of the lattice. Firstly, anti-bend magnets have been utilized to provide additional control over the dispersion function, and an improved symmetrisation in the phase advance between the sextupoles was found to be beneficial for the dynamic aperture. Furthermore, the longitudinal variable bends have been tailored to reduce the emittance and have had transverse gradient added to improve the optics control in the mid-straight sections. In the absence of IDs, the current design provides 161 pm electron beam emittance, reducing to 139 pm once all effects are taken into account. The dynamic aperture is large enough to support an off-axis injection scheme using a nonlinear kicker and has a lifetime greater than 4 h. In this paper the main parameters and magnet specifications for the Diamond-II lattice are provided. The related linear and non-linear beam dynamics issues are discussed, along with the impact of IDs.

INTRODUCTION

The Diamond-II storage ring lattice has been designed using a Modified-Hybrid 6 Bend Achromat structure (M-H6BA). It takes the benefits of both the ESRF 7BA cell [2] and the Diamond DDBA cell [3] and will be placed in the existing storage ring tunnel, keeping the source points fixed. The beam energy has been increased from 3.0 GeV in Diamond to 3.5 GeV in Diamond-II. The optical functions for one super period of the storage ring are shown in Fig. 1 and the corresponding main parameters are given in Table 1. There are 6 long straight sections (LSS) with a length of 7.54 m, 18 standard straight sections (SSS) with a length of 5.06 m (zero dispersion) and 24 low beta mid-straight sections (MSS) with a length of 2.92 m.

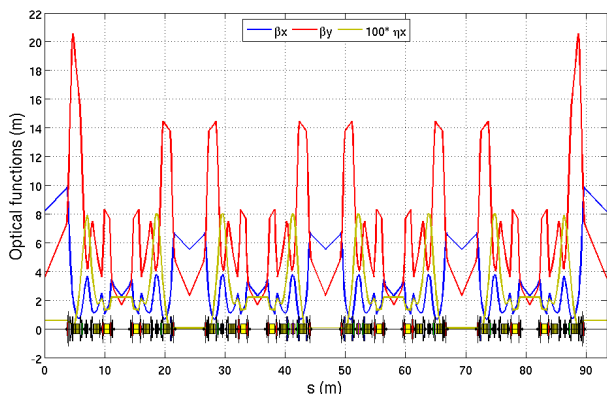


Figure 1: The optical functions along one super period of the Diamond-II storage ring.

[†] Hossein.ghasem@diamond.ac.uk

Table 1: Main Parameters of Diamond-II Storage Ring

Parameter	Value
Energy (GeV)	3.5
Circumference (m)	560.561
Symmetry	6
Tune working point [H, V]	[54.15, 20.27]
Natural emittance (pm)	160.8
Emittance with IDs, IBS, HC (pm)	138.7
Natural chromaticity [H, V]	[-67.5, -88.6]
Energy loss/turn (keV)	723.5
Relative energy spread	9.39×10^{-4}
Momentum compaction	1.04×10^{-4}

MAGNETS

In the Diamond-II M-H6BA lattice structure, each super period consists of four cells. The arrangement of the magnets is shown in Fig. 2 for a standard cell.

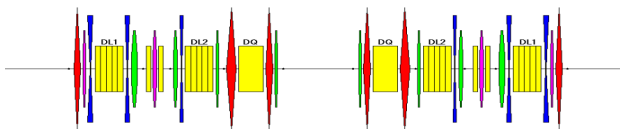


Figure 2: Magnet arrangement in a standard cell.

As shown, there are three main dipoles per half-cell (yellow colour), two of which are longitudinally variable bends (DL1 and DL2) and one a transverse gradient dipole (DQ). The DLs are permanent magnets consisting of five magnet blocks, each of which is 20 cm long and has a different field; the field and transverse gradients are displayed in Fig. 3. The DQ is an electromagnet with field/gradient of 0.695 T/-32.4 T/m.

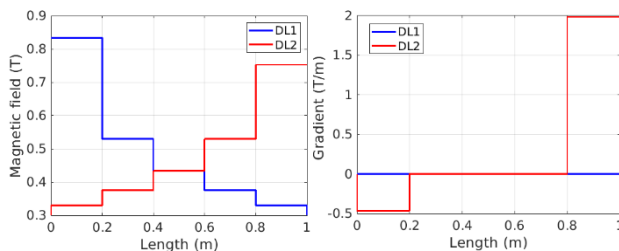


Figure 3: Magnetic field (left) and gradient (right) of the DL dipoles.

The use of two DL dipole types and the addition of transverse gradient is a change from the CDR lattice version [1]. Moreover, two anti-bend quadrupoles have been added between the DLs in the center of dispersion bump of each half cell. To provide the required bend angle of 0.15 deg. at the nominal gradient, the maximum offset is 5.1 mm. In addition to the anti-bend quadrupoles, six normal quadrupoles have been employed for beam focusing. There are also

Content from this work may be used under the terms of the CC BY 3.0 licence (© 2021). Any distribution of this work must maintain attribution to the author(s), title of the work, publisher, and DOI

three chromatic sextupoles in the dispersion bump to correct the natural chromaticity and three harmonic sextupoles with one octupole per half-cell to improve the nonlinear beam dynamic (NLBD) performance.

NLBD OPTIMIZATION STRATEGY

The nonlinear beam dynamic optimization strategy is based on a combination of three phase advance conditions. In the first condition (the -I transformation), the horizontal/vertical phase advance between the central sextupoles in the dispersion bump across the mid-straight section (MSS) is set to $3\pi/\pi$. In the second phase condition (the higher order achromat), the cell tunes have been chosen to cancel the resonance driving terms over 8 cells or two super periods. Small detuning of the phase advance of approximately 0.01 per half-cell has been imposed to avoid major resonances. In the third condition (phase advance symmetrization), considering the different lengths of the straight sections, the strength of the quadrupoles has been optimized to restore the cell symmetry and to provide the same phase advance between the chromatic sextupoles at beginning of different cells up to the 4th decimal place. These phase advance conditions are shown in Fig. 4.

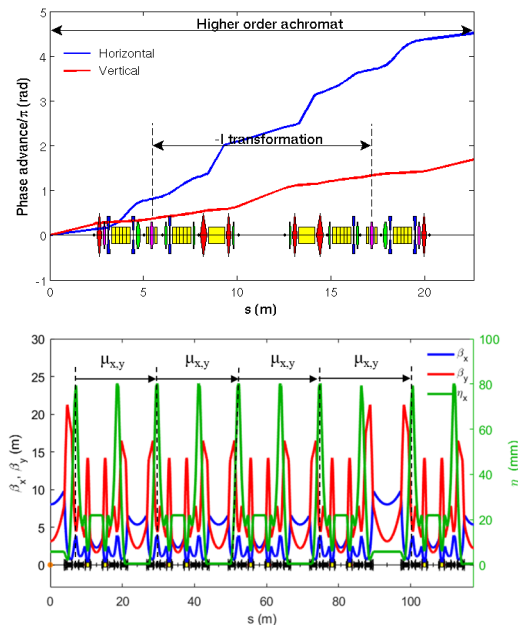


Figure 4: Phase advance conditions in cell, -I transformation and higher order achromat (top) and phase advance symmetrization (bottom).

NON-LINEAR BEAM DYNAMICS

After performing linear beam optics optimization, the natural chromaticity has been corrected using the chromatic sextupoles to positive values and the resonance driving terms have been minimized using the remaining sextupole and octupole families. Particles have been tracked using ELEGANT [4] for 2500 turns to evaluate the dynamic aperture (DA), injection efficiency (IE), momentum aperture (MMAP) and Touschek lifetime. The 4D on and off energy DA with corresponding frequency maps (FM) are

shown in Figs. 5 and 6 respectively. The physical aperture has been included in the tracking. As shown in Fig. 5, the DA is clear of dangerous resonances and is large enough to accommodate efficient off-axis beam injection into the storage ring.

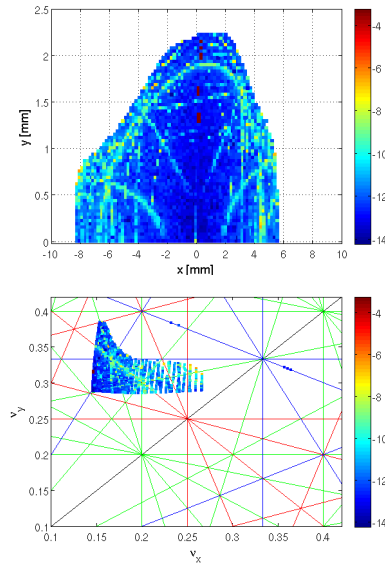


Figure 5: On energy DA (top) and FM (bottom).

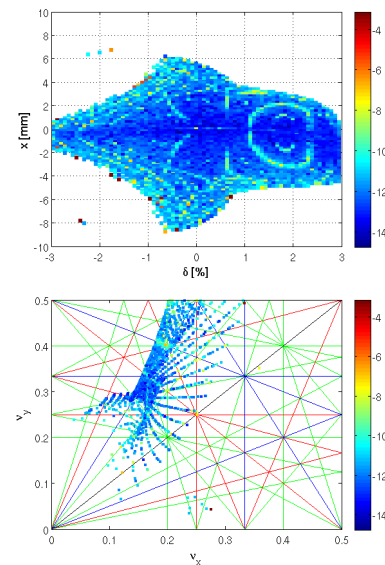


Figure 6: Off energy DA (top) and FM (bottom).

In order to evaluate the injection efficiency (IE), a Gaussian distribution of 1000 particles using the booster parameters [5] has been generated to track through the ring at different amplitudes in the range 0 to 10 mm. Twenty error seeds including strength, misalignment and multipole errors have been imposed, the strength of which have been set to mimic the conditions after full orbit and optics correction. The error amplitudes are given in Table 2. The values quoted are the r.m.s. of a Gaussian distribution which is cut at ± 2 sigma. This fast approximation has been benchmarked against realistic conditions [6]. The IE is shown in Fig. 7. As expected, injection at small amplitudes is 100% efficient. Looking at the average curve shown with a thick

blue line with error bars, the IE at -5 mm in Diamond-II is more than 95%. This compares well with the proposed injected beam amplitude of -3.5 mm giving confidence a high IE can be achieved.

Table 2: Errors used to Simulate the Corrected Machine

Lifetime	Value
Magnet misalign./roll ($\mu\text{m}/\mu\text{rad}$)	15/100
BPM misalign./roll ($\mu\text{m}/\mu\text{rad}$)	10/10
Dipole/Quad./Sext./Oct. fractional strength error	$10^{-4}/10^{-3}/10^{-3}/10^{-3}$

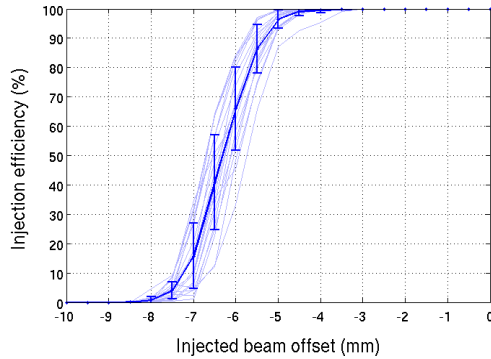


Figure 7: Injection efficiency as function of amplitude.

INSERTION DEVICES

In total there will be 34 insertion devices (IDs) in the Diamond-II storage ring, the majority of which will be re-used from Diamond-I. These include several new and re-located beamlines in the additional MSS. The finite dispersion of these straights will lead to a small increase in the emittance and energy spread when the IDs are closed. This partially offsets the reduction found when operating the IDs in the low dispersion LSS and SSS (particularly the two superconducting wigglers (SCW)).

The IDs are also found to affect the linear and nonlinear beam dynamics. Local correction techniques such as alpha matching will be employed for the SCWs as currently in Diamond [7]. For the proposed I05 APPLE-KNOT undulator, active shims are being considered [8]. Alpha-matching has been found to be effective in all types of straights, including when using quadrupoles within the achromat. The effect of IDs in the MSS is small and even helps to achieve the -I condition. Detailed studies of ID effects are underway and no problems in operating Diamond-II are foreseen.

LIFETIME

The overall lifetime in the storage ring is based on a combination of different scattering processes such as quantum scattering, Touschek scattering, elastic and inelastic gas scattering. The dominant scattering process is the Touschek effect which scales with the momentum aperture. When calculating the MMAP for the storage ring, the RF cavity has been set to its optimized voltage in the absence of IDs of 1.42 MV. The momentum aperture for one super period of the ring is plotted in Fig. 8. As can be seen, the

momentum aperture is $\pm 1.8\%$ in the arcs and $\pm 3\%$ in the straight sections.

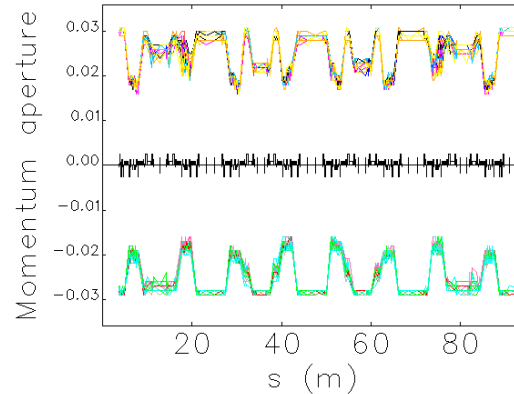


Figure 8: Momentum aperture for one super-period.

Taking 8 pm for the vertical emittance and 0.6 nC for the bunch charge (corresponding to a beam current of 300 mA), the average Touschek lifetime over 20 ensembles is found to be 1.8 h. The gas lifetime is evaluated using the average DA and MMAP in the ring. A uniform pressure of 0.75 nTorr with 100% CO has been assumed. The effect of a 3rd harmonic cavity (HC) has been approximated by increasing the natural bunch length ($\sigma_l = 3.75$ mm) by a factor three. A summary of the lifetime components is given in Table 3.

Table 3: Contributions to the Storage Ring Lifetime

Lifetime	Value
Touschek (h)	1.80±0.12
Coulomb (h)	48.99
Bremsstrahlung (h)	73.56
Total gas (h)	29.41
Average Touschek with IDs, IBS, HC (h)	5.04
Overall lifetime (h)	4.3

ONGOING WORK

Multi-objective Genetic Algorithm (MOGA) optimisation of the lattice and tune-scans are underway with the aim of maximising lifetime and dynamic aperture. Starting from the baseline lattice and without changing the hardware, we are also investigating potential future operating modes with an emittance of ~ 100 pm and with beta functions matched to the photon beam at the straight sections to maximise the brightness. Lastly, a beam collimation strategy is currently being developed.

ACKNOWLEDGEMENTS

The authors would like to thank all former colleagues, particularly M. Apollonio, R. Bartolini and J. Bengtsson for their valued contributions.

REFERENCES

- [1] C. Abraham, L. Alianelli, *et al.*, “Diamond-II Conceptual Design Report”, Oxfordshire, UK, Rep. Diamond-II, 2019.

- [2] D. Andrault *et al.*, “ESRF Upgrade Program Phase II (Orange Book)”, ESRF, Grenoble, France, Rep. ESRF, 2014.
- [3] I. P. S. Martin, R. Bartolini, M. Apollonio, R. T. Fielder, and E. Koukovini-Platia, B. Singh, “Characterization of the double-double bend achromat lattice modification to the Diamond Light Source storage ring”, *Phys. Rev. ST Accel. Beams*, vol. 21, p. 060701, 2018.
doi:10.1103/PhysRevAccelBeams.21.060701
- [4] M. Borland, “elegant: a flexible sdds-compliant code for accelerator simulation”, Advanced Photon Source, Argonne National Laboratory, Lemont, IL, USA, Report No. LS-287, 2000.
- [5] I. P. S. Martin *et al.*, “Progress with the Booster Design for the Diamond-II Upgrade”, presented at Proc. IPAC’21, Campinas, Brazil, May 2021, paper MOPAB071, this conference.
- [6] M. Apollonio, *et al.*, “Commissioning Strategy for Diamond-II”, presented at IPAC’21, Campinas, Brazil, May 2021, paper MOPAB063, this conference.
- [7] B. Singh *et al.*, “Commissioning and Investigation of Beam Dynamics of Phase-I Insertion Devices at Diamond”, in *Proc. PAC’07*, Albuquerque, New Mexico, USA, Jun. 2007, paper TUPMN088, pp. 1118-1120.
- [8] I. P. S. Martin *et al.*, “Active Optics Stabilisation Measures at the Diamond Storage Ring”, in *Proc. IPAC’14*, Dresden, Germany, Jun. 2014, pp. 1760-1762.
doi:10.18429/JACoW-IPAC2014-TUPRI082